Laser-induced magnetisation dynamics in $La_{0.7}Sr_{0.3}MnO_3$/$SrRuO_3$ superlattices

Ilya Razdolski[*,1], Ruslan R. Subkhangulov[1], Diana G. Gheorghe[1], Francis Bern[2], Ionela Vrejoiu[3], Alexey V. Kimel[1], Andrei Kirilyuk[1], Michael Ziese[2], Theo Rasing[1]

[1] Radboud University Nijmegen, Institute for Molecules and Materials, 6525 AJ Nijmegen, The Netherlands
[2] Division of Superconductivity and Magnetism, University of Leipzig, D-04103 Leipzig, Germany
[3] Max Planck Institute for Solid State Research, Heisenbergstr. 1, D-70569 Stuttgart, Germany

Received XXXX, revised XXXX, accepted XXXX
Published online XXXX

Key words: Magnetisation dynamics, time-resolved Kerr rotation, complex oxides, superlattice, multilayer

[*] Corresponding author: e-mail: razdolski@fhi-berlin.mpg.de, Present Address: Fritz-Haber-Institut der MPG, Faradayweg 4-6, 14195 Berlin, Germany; Phone: +49-30-84135114, Fax: +49-30-84135106

Laser-induced magnetisation dynamics of a $La_{0.7}Sr_{0.3}MnO_3$/ $SrRuO_3$ superlattice is studied by means of a single-colour optical pump-probe technique. Significant differences in the magnetisation dynamics of a superlattice with respect to the single layers of constituent materials are demonstrated. Below the Curie temperature T_C of $SrRuO_3$, laser-induced ultrafast demagnetisation is found to be followed by a uniform precession of the magnetisation around its new equilibrium. The data is described within a simple model based on a displacive excitation of a precessional magnetisation dynamics. The model is shown to give a good fit to the experimental data. As the initial temperature approaches T_C, the oscillations get suppressed and eventually vanish. The magnetisation dynamics is shown to depend on whether the two distinct magnetisation vectors in the superlattice are ferromagnetically or antiferromagnetically aligned.

1 Introduction Complex ferromagnetic oxides demonstrate a large variety of interesting physical properties, which can become truly peculiar at the interfaces [1–5]. Generally, manganites, as well as other perovskite magnetic materials, allow subtle changes of their magnetic properties by means of cation doping [6–8]. In order to exploit the interface properties of these materials, multilayer thin films are often studied [9–11], as they are capable of providing a much stronger interface response, as compared to thick homogeneous samples. For instance, a heterostructure consisting of two magnetic layers often exhibits an exchange interaction across the interface, leading to the appearance of exchange bias which results in pinning of the magnetisation of the softer magnetic material by the harder one [12–15]. Another interesting feature which is facilitated by the interface exchange is the existence of an interfacial (two-dimensional) gas of free carriers, which has been demonstrated by means of Hall and transport measurements, as well as direct structural imaging [16–19].

Obviously, an outstanding crystalline quality of the layers is needed in order to achieve these properties, which can be obtained in manganite/ruthenate samples. The similar lattice constants of this whole family of materials are highly beneficial from the point of view of growth of high-quality heterostructures with epitaxial atomic-abrupt interfaces. One of the finest examples of these heterostructures is the $\{La,Sr\}MnO_3$/$SrRuO_3$ superlattice, studied extensively in [17] and References therein. In particular, this manganite/ruthenate superlattice of magnetically soft (manganite) and hard (ruthenate) layers is considered to be a model system for the study of interface properties of strongly correlated materials. Although the static magnetic properties of these structures are quite well known, little is

understood regarding the details of highly non-equilibrium light-matter interactions that result from femtosecond optical excitation [20]. These studies are of great interest in the light of recent development of optical laser-induced magnetisation switching in superlattices [21].

In fact, there exists an number of papers discussing excitation and dynamics of the magnetization in exchange-biased [22–24] or exchange-coupled [25,26] multilayer structures. In this paper, we study the magnetisation dynamics of a superlattice of two ferromagnetic oxides, which are coupled antiferromagnetically by means of the exchange interaction, driven by a femtosecond laser pulse. The two components of the superlattice are of a very different nature: the itinerant ferromagnet $SrRuO_3$ is coupled to the colossal-magnetoresistive $La_{0.7}Sr_{0.3}MnO_3$. Because of very dissimilar electronic structures, ultrafast magnetization dynamics is expected to be very unalike in the two components. We analyse the collective response of the $La_{0.7}Sr_{0.3}MnO_3/SrRuO_3$ superlattice and show that the equilibrium of the magnetisations of the two sublattices can be destroyed on the ultrafast timescale, which triggers magnetisation precession. We discuss the mechanism of the excitation of this precession and analyse it using a two-sublattice model, which allows us to describe the experimentally observed dependence upon changing the external magnetic field. We analyse the timescales of the magnetisation dynamics and study their temperature dependence in the vicinity of the T_C of the magnetically hard $SrRuO_3$.

2 Sample characterisation In our work we studied a superlattice of 15 $La_{0.7}Sr_{0.3}MnO_3/SrRuO_3$ bilayers grown by pulsed laser deposition on a vicinal $SrTiO_3(001)$ substrate. The thicknesses of the $La_{0.7}Sr_{0.3}MnO_3$ and $SrRuO_3$ were 2.3 and 3.2 nm, respectively. The interlayer coupling is antiferromagnetic below the T_C of $SrRuO_3$ (about 145 K) [11], which results in a large exchange bias of 4 T for the $SrRuO_3$ magnetisation hysteresis loop. In this structure, the magnetisation of $La_{0.7}Sr_{0.3}MnO_3$ layers is the strongest and thus is aligned along the external magnetic field, if the latter is applied in the sample plane. The $SrRuO_3$ magnetisation points thus in the opposite direction. If the magnetic field H is tilted from the in-plane configuration, the equilibrium condition is determined by an interplay of this field, the superexchange interaction via the Mn-O-Ru route across the interfaces [11,27] and the magnetic anisotropy of both types of layers.

2.1 Static properties In order to understand the origin of the magneto-optical signal from the sample (see below), we performed magneto-optical Kerr effect (MOKE) measurements on the superlattice, as well as on single films of the constituting materials. The thicknesses were chosen to match those of the single layers in the superlattice, that is, 2.3 and 3.2 nm. In the static MOKE measurements, the magnetic field was applied in-plane by an electromagnet. The schematic of the experimental setup is sketched in Fig.1,a, where the antiferromagnetic alignment of the magnetisations in the superlattice is also illustrated. The results of the MOKE measurements for a temperature of 80 K are shown in Fig.1,b, where the cw laser radiation with a wavelength of 633 nm was used as a probe.

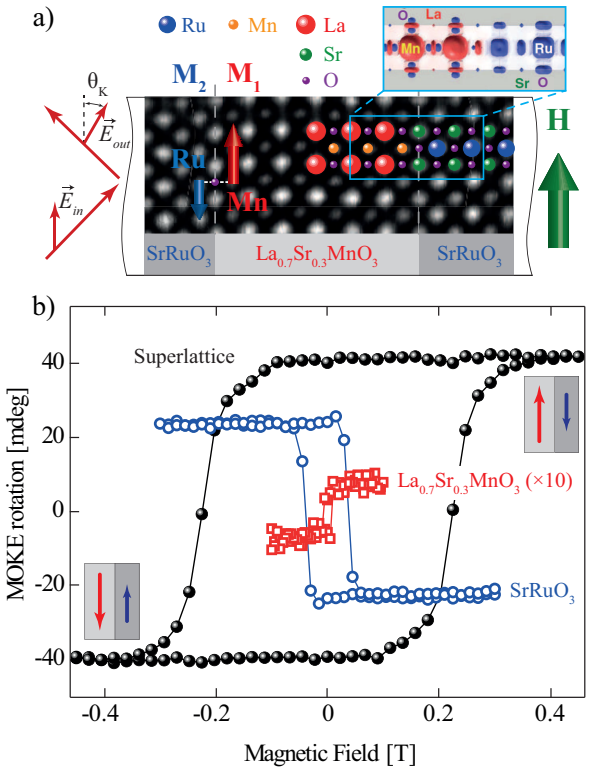

Figure 1 (a) Scheme of the static MOKE measurement and structure of the superlattice. Red and blue arrows correspond to the magnetisation directions of the $La_{0.7}Sr_{0.3}MnO_3$ and $SrRuO_3$ layers, respectively. The crystalline structure image was obtained with scanning transmission electron microscopy (STEM). Inset shows the spin density at the interfaces, adapted from [11] (b) Magnetic hysteresis measured by MOKE for the superlattice (black full dots) and single films (blue open dots and red open squares) of corresponding materials. The insets illustrate the magnetic state of the superlattice at saturating fields of opposite directions.

The multilayer hysteresis loop shown in Fig. 1,b reproduces the inner loop from Ref. [13] and corresponds to the inversion of both magnetisations in the multilayer, while keeping their mutual antiferromagnetic alignment. It is clearly seen that the magneto-optical response of the superlattice is dominated by the magnetic moments of the $SrRuO_3$ layers. The latter was also confirmed as the MOKE signal disappeared at temperatures above the T_C of $SrRuO_3$. The origin of the large magneto-optical activity of $SrRuO_3$ is believed to be the strong spin-orbit coupling of the ruthenium atoms [28,29]. Moreover, it is seen that the sign of the MOKE hysteresis loop from the single $SrRuO_3$

is different from that of the superlattice. This confirms the antiferromagnetic alignment of the magnetisations of the two types of layers and the dominating role of the $La_{0.7}Sr_{0.3}MnO_3$ layers with respect to the $SrRuO_3$ ones regarding the magnetisation orientation. Thus, in the superlattice the larger magnetic moment of the $La_{0.7}Sr_{0.3}MnO_3$ layers governs the magnetisations orientation with respect to the external in-plane field, while the magnetisation of the $SrRuO_3$ layers, aligned antiparallel to the external field, largely determines the total magneto-optical signal due to their much larger magneto-optical susceptibility.

2.2 Magnetisation dynamics in single films For the pump-probe measurements we used an amplified laser system capable of producing 60 fs pulses with a repetition rate of 1 kHz in the near-infrared spectral range. In the experiment, laser radiation with a wavelength of 800 nm was used for both pump and probe beams, focussed on the sample into spots of approximately 400 and 200 microns in diameter, respectively. The angle of incidence of the pump and probe beams was about 45 and 50 degrees, respectively. The pump fluence was kept at a moderate level of 7 mJ/cm^2. The fluence ratio between the two linearly polarised beams was below 0.01, so that the effect of the probe beam on the magnetic state of the sample could be considered negligible. The samples were placed in a superconducting split coil magneto-optical cryostat in an external magnetic field. Unlike for the static measurements, the external magnetic field was applied at an angle of 45 degrees with respect to the sample plane. The rotation of the polarisation plane of the radiation reflected from the sample was registered with the balance detection scheme. Each dataset shown below was measured for two opposite fields H_+,H_- and the plotted value θ was obtained as $\theta = \theta(H_+) - \theta(H_-)$. This has been done in order to remove all the contributions to the rotation of the polarisation plane of the probe beam which have a non-magnetic origin. Further, $\theta(H_+) + \theta(H_-)$ signals do not show any interesting dynamics and will not be discussed below.

For the further characterisation of the sample we performed pump-probe experiments on the $La_{0.7}Sr_{0.3}MnO_3$ and $SrRuO_3$ films, both grown on the $SrTiO_3$ substrate under the same conditions as the superlattice. The result shown in Fig.2 demonstrates drastic differences in the timescales of the initial demagnetisation. Whereas the magnetisation of $SrRuO_3$ is quenched after just a few ps, it takes a few hundreds of picoseconds to demagnetise the $La_{0.7}Sr_{0.3}MnO_3$ film. We note that this observation is consistent with the previous works on these and similar materials [30–33]. No oscillatory behaviour of the magnetisation was found in a wide range of applied external fields (from 1 up to 6 T), indicating that the anisotropy fields H_a are relatively small, and the equilibrium direction of the magnetisation coincides with the applied external field. In these conditions, laser-induced effects such as demagnetisation and anisotropy quenching are incapable of exciting precessional dynamics of the magnetisation.

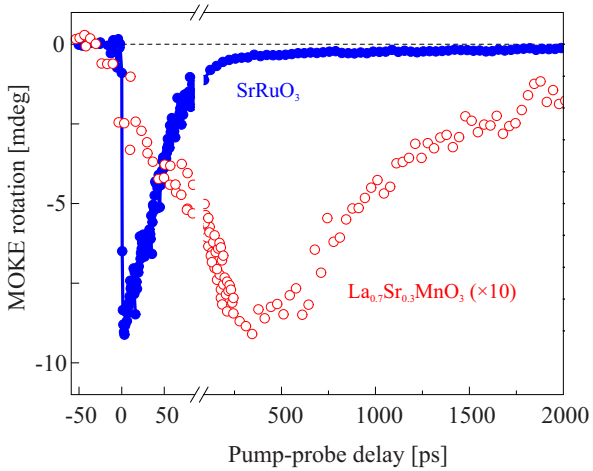

Figure 2 Magnetisation dynamics of the single films of SRO (blue closed symbols) and LSMO (red open symbols) at 80 K in the external field of 3 T.

3 Magnetisation dynamics in a superlattice Now we turn to the superlattice consisting of the $La_{0.7}Sr_{0.3}MnO_3$ and $SrRuO_3$ layers. Its magnetisation dynamics on the timescale of tens of picoseconds is shown in Fig.3,a,b for two values of the external magnetic field, 3 and 6 T. These values correspond to *antiferromagnetic* and *ferromagnetic* alignment of the magnetisations in the superlattice, respectively (see discussion on Fig. 1 and Ref. [13]). One can see a fast modulation of the MOKE signal (on the scale of 1-2 ps), which is probably associated with the optical state-filling effect [34]. This effect, accompanying the laser-induced demagnetization, has a short lifetime and will not be further discussed here. It is also seen (Fig.3,a) that at lower temperatures the demagnetisation is followed by oscillations associated with the precession of the magnetisation. This precession is absent at temperatures of 110 K and higher. In what follows we shall discuss the nature of this oscillatory dynamics and demonstrate the mechanism responsible for its optical excitation on the ultrafast timescale.

4 Discussion Figure 4 illustrates the transient MOKE rotation θ measured at 80 K for several values of the external magnetic field H. It is seen that the oscillations frequency increases with the strength of the applied magnetic field. On the other hand, the frequency was found to be independent of the temperature in the range from 10 K up to 90 K. No dependence of the oscillations on the polarisation of the pump beam (in the plane of incidence or perpendicular to it) was registered. The data were fitted with the decaying oscillations function starting at the zero time delay.

These experimental observations, together with the absence of oscillations at higher temperatures, suggest that the mechanism for the excitation of the magnetisa-

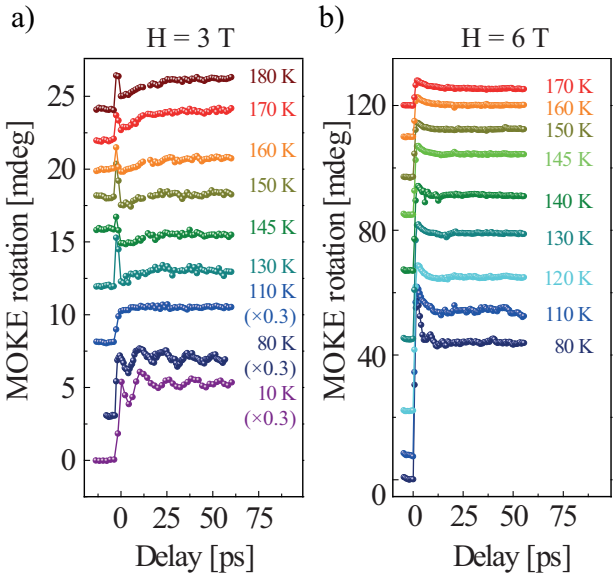

Figure 3 Temperature dependence of the transient MOKE signal for an external field of (a) 3 T and (b) 6 T, corresponding to the antiferromagnetic and ferromagnetic alignment of the magnetisations in the superlattice, respectively.

tion precession is based on laser-induced demagnetisation of the sample. As the Curie temperature of the $SrRuO_3$ $T_C \approx 145$ K is much lower than that of $La_{0.7}Sr_{0.3}MnO_3$ (320 K) [17], it is natural to assume that the laser-induced demagnetisation acts more severely on the $SrRuO_3$ layers. Thus the absence of oscillations is attributed to the complete demagnetisation of the $SrRuO_3$ layers due to the laser-induced heating. The apparent increase of the damping of the oscillations when increasing the external field up to 6 T is associated with a transition to a state in which the magnetisations are ferromagneticly aligned, which may also alter the dynamic properties of the multilayer.

The mechanism of the excitation of coherent precession of magnetisation can be described in the following way. Since the magnetic field H is applied at an angle of 45 degrees with respect to the sample plane, the equilibrium directions of both magnetisations M_1, M_2 (corresponding to the $La_{0.7}Sr_{0.3}MnO_3$ and $SrRuO_3$ layers, respectively) is determined by an interplay of this field H, the exchange interaction between M_1 and M_2 and the (low) magnetic anisotropy of the layers. Once the magnetisation M_2 is partly quenched by the pump pulse, the equilibrium conditions are changed, and a torque is exerted on what is left from M_2. The latter finds itself out of the equilibrium and starts to precess until the magnetisation (and anisotropy) is restored. Note that a similar mechanism for the excitation of the spin precession in *ferromagnetically* coupled superlattices was proposed in [20]. Of course, the equilibrium condition for M_1 is also changed, and the two magnetisations oscillate together. However, due to the low magneto-optical sensitivity to the magnetisation of $La_{0.7}Sr_{0.3}MnO_3$ (see Fig.1) this dynamics is not detectable in our experiments.

We can write down the free energy for a bilayer $La_{0.7}Sr_{0.3}MnO_3$/ $SrRuO_3$, assuming that its magnetic properties are identical to those of the superlattice:

$$F = -\mathbf{H}\cdot\mathbf{M_1} - \mathbf{H}\cdot\mathbf{M_2} + \lambda\mathbf{M_1}\cdot\mathbf{M_2} + F_{a1} + F_{a2} \quad (1)$$

Here λ is the exchange interaction constant between M_1 and M_2, and the last two terms represent the energy related to the magnetocrystalline anisotropy. In the case of thin films, when the in-plane direction is favourable, they can be written as $F_{ai} = M_i H_{ai} \cos^2\theta_i$, where H_{ai} are the anisotropy fields, θ_i are the angles between the z-axis normal to the sample and the magnetisation M_i (see also Fig.4,b), $i = 1, 2$. As a next step, effective fields can be found and the system of Landau-Lifshitz equations [35] yields the eigenfrequencies f_j of the system as a function of the external field H, if we know the initial equilibrium conditions. In the equilibrium, the magnetisations $\mathbf{M_i}$ make angles θ_{10}, θ_{20} with the z-axis, *i.e.* the direction normal to the sample surface (Fig. 4,b). These angles θ_{10}, θ_{20} can be found from $\frac{\partial F}{\partial \theta_i} = 0$.

When the sample is exposed to a laser pulse, laser-induced demagnetisation occurs on the ultrafast timescale, as a result of the thermalisation of the heated electrons with the spins. As noted above, we can safely restrict ourselves to the demagnetisation of the $SrRuO_3$ layers only. Our measurements of $SrRuO_3$ single films indicate this happens within the first picoseconds after the laser excitation, which is also in accordance with the literature [30,31, 33]. The anisotropy field H_{a2} also decreases. Both of these effects displacively shift the equlibrium angle for the magnetisations M_1, M_2, and the system finds itself precessing around the new equilibrium angles θ_1', θ_2'. These can be found by solving the same system with the new values of the H_{ai}, M_i coefficients.

As such, we can estimate the amplitude of the precession by simply taking the difference between the old and new equilibrium angles $\theta_{i0} - \theta_i'$ as a function of the external field H and compare it to the experimental data. Here again we only consider angles θ_2 (related to the $SrRuO_3$), as they are the only ones which are detected in the experiment. The best fit for the temperature of 80 K is shown in Fig.4,c, top panel, and was obtained for a demagnetisation of about 50%. This is a reasonable value given that the T_C of $SrRuO_3$ (≈ 145 K) is relatively close. The non-monotonous amplitude dependence on the external magnetic field can be understood invoking the shape anisotropy of the films, which favours the in-plane direction of the magnetizations for both materials. This anisotropy is about 0.5 T, comparable to the normal projection of the external magnetic field, at which the largest amplitude of the oscillations is observed. The influence of this anisotropy is also

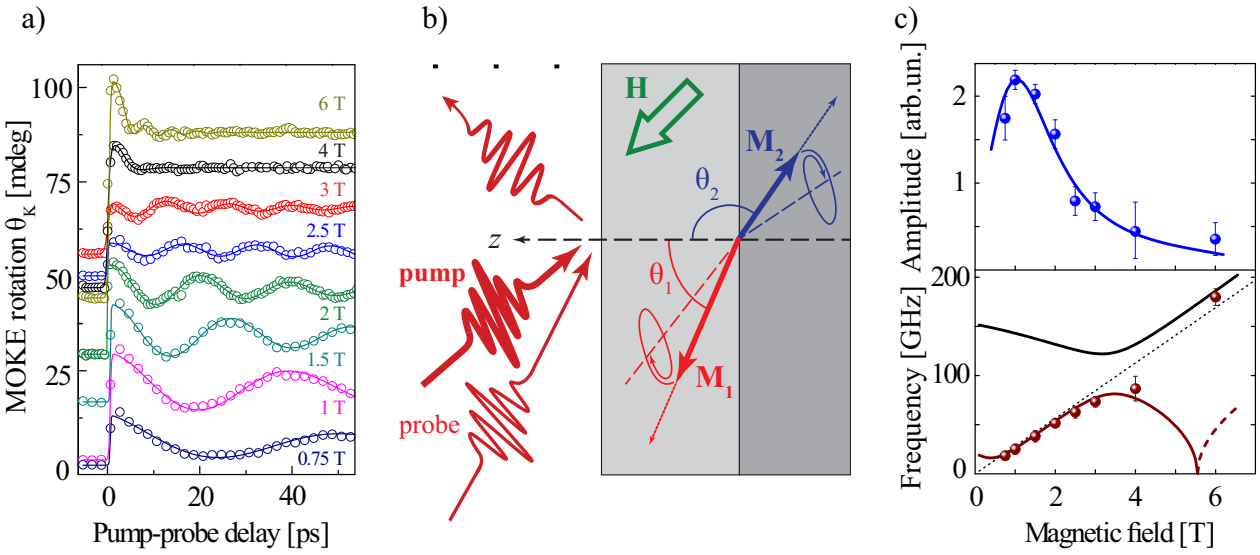

Figure 4 (a) Transient MOKE signal measured at 80 K for various magnetic fields (open dots) and the fits to the data with the decaying oscillations (solid lines). (b) Mechanism of the excitation of the magnetisation precession: Thick solid arrows represent the quenched magnetic moments right after the ultrafast demagnetisation, and dashed lines show the new equilibrium directions for both magnetisations. (c) Experimental data (points) and fit (solid line) for the dependence of the amplitude (top) and frequency (bottom) of the oscillations in MOKE signal on the strength of the external magnetic field. The dashed line in (c) shows the result expected for the free electron spin precession.

seen in Fig. 4,c, bottom panel, at small fields (below 0.5 T).

For the same set of parameters the frequency dependence on the magnetic field is shown in Fig.4,c, bottom panel, giving a good agreement with the experimental data too. The relatively large error bar at 4 T is caused by a very quick damping of the oscillatory dynamics and the uncertainty of the fit parameters associated with it. The system of Landau-Lifshitz equations in a two-sublattice magnetic system has two solutions [36, 37], which are shown in Fig. 4,c, bottom panel, with black and dark red solid lines. These two modes exhibit a pronounced avoided crossing behaviour. Note that in large magnetic fields (such as 6 T) the SRO and LSMO magnetisations are aligned parallel to each other. As such, the only mode present in these conditions is the simultaneous precession of both magnetisations, which is why above 6 T the dashed part of the dark red line does not correspond to any real physical process. The thin black dotted line there represents the expected dependence for the free electron spin precession with the slope of 28.2 GHz/T.

In addition to that, the high-frequency oscillations in the $SrRuO_3$ single films reported in [31, 33] were not observed. Further, no magnetisation precession was found in the experiments on the single $SrRuO_3$ and $La_{0.7}Sr_{0.3}MnO_3$ films (see Fig.2), probably due to the following reason. For excitation mechanism proposed it is crucial that the thickness of the $SrRuO_3$ film is above a certain threshold which is about 15 unit cells [15, 17]. Then the magnetocrystalline anisotropy in the bulk of $SrRuO_3$ leads to the easy magnetisation axis at some angle with respect to the sample plane. This angle was found to be temperature-dependent, thus shifting the equilibrium condition for the magnetisation upon laser-induced heating. In our superlattice, the $SrRuO_3$ layers are thin enough and the easy-axis is always in-plane, which (without applying an additional external out-of-plane field) makes the aforementioned excitation mechanism irrelevant. On the longer timescale the $SrRuO_3$ magnetisation demonstrates no precessional behaviour, in agreement with the previously reported data [30].

5 Conclusions To summarise, we have studied laser-induced magnetisation dynamics in a superlattice of 15 $La_{0.7}Sr_{0.3}MnO_3/SrRuO_3$ bilayers, as well as in single films, by means of optical pump-probe experiments. At low temperatures, we have found that the femtosecond laser excitation can displacively trigger coherent magnetisation dynamics. We demonstrated that this coherent dynamics is absent in the single films of the constituent materials and can only be excited in superlattices. We propose a mechanism, where an ultrafast partial demagnetisation of $SrRuO_3$ instantly shifts the equilibrium angle of magnetisation and the newly appeared torque starts the precession. For the said mechanism the role of the superexchange Ru-O-Mn interaction across the interface is truly crucial. The oscillations cease to start at temperatures above 90 K, which is related to the total demagnetisation of the $SrRuO_3$ layers. This model allowed us to obtain a good fit for the dependences of both frequency and amplitude of

the oscillations as a function of the external magnetic field strength.

Acknowledgements The authors would like to thank Dr. E. Pippel, MPI of Microstructure Physics, Halle, Germany, for the STEM characterization of the sample. This work has been supported by the 7th Framework Program (EU-FP7) Grant Nr. NMP-3-LA-2010-246102 (IFOX Project) and the European Research Council ERC Grant agreement No. 257280 (Femtomagnetism) and No. 339813 (Exchange).

References

[1] J.-H. Park, E. Vescovo, H.-J. Kim, C. Kwon, R. Ramesh, T. Venkatesan, Nature **392**, 794 (1998).
[2] J. A. Bert, B. Kalisky, C. Bell, M. Kim, Y. Hikita, H. Y. Hwang, K. A. Moler, Nat. Phys. **7**, 767 (2011).
[3] D. A. Dikin, M. Mehta, C.W. Bark, C. M. Folkman, C. B. Eom, V. Chandrasekhar, Phys. Rev. Lett. **107**, 056802 (2011).
[4] M. Gibert, P. Zubko, R. Scherwitzl, J. Iniguez, J.-M. Triscone, Nat. Mater. **11**, 195 (2012).
[5] Y. M. Sheu, S. A. Trugman, L. Yan, Q. X. Jia, A. J. Taylor, R. P. Prasankumar, Nat. Commun. **5**, 5832 (2014).
[6] G. H. Jonker, J. H. van Santen, Physica **XVI(3)**, 337 (1950).
[7] W. Lee, J. W. Han, Y. Chen, Z. Cai, B. Yildiz, J. Am. Chem. Soc. **135**, 7909 (2013).
[8] Y. Murakami, J. H. Joo, D. Shindo, T. Atou, M. Kikuchi, Nature **423**, 965 (2003).
[9] C. v. Korff Schmising, M. Bargheer, M. Kiel, N. Zhavoronkov, M. Woerner, T. Elsaesser, I. Vrejoiu, D. Hesse, M. Alexe, Phys. Rev. B **73**, 212202 (2006).
[10] F. Y. Bruno, J. Garcia-Barriocanal, M. Varela, N. M. Nemes, P. Thakur, J. C. Cezar, N. B. Brookes, A. Rivera-Calzada, M. Garcia-Hernandez, C. Leon, S. Okamoto, S. J. Pennycook, J. Santamaria, Phys. Rev. Lett. **106**, 147205 (2011).
[11] M. Ziese, I. Vrejoiu, E. Pippel, P. Esquinazi, D. Hesse, C. Etz, J. Henk, A. Ernst, I. V. Maznichenko, W. Hergert, I. Mertig, Phys. Rev. Lett. **104**, 167203 (2010).
[12] X. Ke, M. S. Rzchowski, L. J. Belenky, C. B. Eom, Appl. Phys. Lett. **84**, 26, 5458 (2004).
[13] M. Ziese, I. Vrejoiu, D. Hesse, Appl. Phys. Lett. **97**, 052504 (2010).
[14] P. Padhan, W. Prellier, R. C. Budhani, Appl. Phys. Lett. **88**, 192509 (2006).
[15] J.-H. Kim, I. Vrejoiu, Y. Khaydukov, T. Keller, J. Stahn, A. Rühm, D. K. Satapathy, V. Hinkov, B. Keimer, Phys. Rev. B **86**, 180402 (2012).
[16] A. Ohtomo, H. Y. Hwang, Nature **427**, 423 (2004).
[17] M. Ziese, I. Vrejoiu, Phys. Status Solidi RRL **7(4)**, 243 (2013).
[18] M. Ziese, F. Bern, E. Pippel, D. Hesse, I. Vrejoiu, Nano Lett. **12**, 4276 (2012).
[19] A. Y. Borisevich, A. R. Lupini, J. He, E. A. Eliseev, A. N. Morozovska, G. S. Svechnikov, P. Yu, Y.-H. Chu, R. Ramesh, S. T. Pantelides, S. V. Kalinin, S. J. Pennycook, Phys. Rev. B **86**, 140102 (2012).
[20] H. B. Zhao, K. J. Smith, Y. Fan, G. Lüpke, A. Bhattacharya, S. D. Bader, M. Warusawithana, X. Zhai, J. N. Eckstein, Phys. Rev. Lett. **100**, 117208 (2008).
[21] S. Mangin, M. Gottwald, C-H. Lambert, D. Steil, V. Uhl, L. Pang, M. Hehn, S. Alebrand, M. Cinchetti, G. Malinowski, Y. Fainman, M. Aeschlimann, and E. E. Fullerton, Nat. Mater. **13**, 286 (2014).
[22] G. Ju, A. V. Nurmikko, R.F.C. Farrow, R.F. Marks, M.J. Carey, and B.A. Gurney, Phys. Rev. Lett. **82**, 3705–3708 (1999).
[23] A. Porat, S. Bar-Ad, and I.K. Schuller, Eur. Phys. Lett. **87**, 67001 (2009).
[24] F. Dalla Longa, J.T. Kohlhepp, W.J.M. de Jonge, and B. Koopmans, Phys. Rev. B **81** 094435 (2010).
[25] R. Adam, P. Grychtol, S. Cramm, and C.M. Schneider, J. Electron Spectrosc. Relat. Phenom. **184**, 291–295 (2011).
[26] D. Rudolf, C. La-O-Vorakiat, M. Battiato, R. Adam, J.M. Shaw, E. Turgut, P. Maldonado, S. Mathias, P. Grychtol, H.T. Nembach, T.J. Silva, M. Aeschlimann, H.C. Kapteyn, M.M. Murnane, C.M. Schneider, and P.M. Oppeneer, Nat. Comm. **3**, 1037 (2012).
[27] Y. Lee, B. Caes, B. N. Harmon, J. Alloys Compd. **450**, 1 (2008).
[28] L. Klein, J. S. Dodge, T. H. Geballe, A. Kapitulnik, A. F. Marshall, L. Antongazza, K. Char, Appl. Phys. Lett., **66(18)**, 2427 (1995).
[29] G. Herranz, N. Dix, F. Snchez, B. Martnez, J. Fontcuberta, M. V. Garcia-Cuenca, C. Ferrater, M. Varela, D. Hrabovsky, A. R. Fert, J. Appl. Phys. **97**, 10M321 (2005).
[30] T. Ogasawara, K. Ohgushi, Y. Tomioka, K. S. Takahashi, H. Okamoto, M. Kawasaki, Y. Tokura, Phys. Rev. Lett. **94**, 087202 (2005).
[31] M. C. Langner, C. L. S. Kantner, Y. H. Chu, L. M. Martin, P. Yu, J. Seidel, R. Ramesh, J. Orenstein, Phys. Rev. Lett. **102**, 177601 (2009).
[32] G. M. Müller, J. Walowski, M. Djordjevic, G.-X. Miao, A. Gupta, A. V. Ramos, K. Gehrke, V. Moshnyaga, K. Samwer, J. Schmalhorst, A. Thomas, A. Hütten, G. Reiss, J. S. Moodera, M. Münzenberg, Nat. Mater. **8**, 56 (2009).
[33] C. L. S. Kantner, M. C. Langner, W. Siemons, J. L. Blok, G. Koster, A. J. H. M. Rijnders, R. Ramesh, J. Orenstein, Phys. Rev. B **83**, 134432 (2011).
[34] B. Koopmans, M. van Kampen, J. T. Kohlhepp, and W. J. M. de Jonge, Phys. Rev. Lett. **85**, 844–847 (2000).
[35] L. D. Landau and E. M. Lifshitz, *Statistical Physics*, Part 2 (Pergamon Press, New York, 1980).
[36] A. S. Borovik-Romanov, S. O. Demokritov, N. M. Kreines, and V. I. Kudinov, JETP **61**, 801 (1985).
[37] R. R. Subkhangulov, A. B. Henriques, P. H. O. Rappl, E. Abramof, Th. Rasing, and A. V. Kimel, Sci. Rep. **4**, 4368 (2013).